Electronic Supplementary Information

Highly emissive blue graphene quantum dots with excitation-independent emission via ultrafast liquid-phase photoreduction

Jae-Won Lee, [a,b] Ji Hye Kwak, [c] Juhee Kim, [b] Yoon-Kwan Jang, [d] Joong Tark Han, [b] Tae-Jin Kim, [d] Kyong-Soo Hong, [e] Hee Jin Jeong, *[b] Imjeong H.-S Yang *[a]

[a]*Department of Physics, Pusan National University, Busan 46241, South Korea*
[b]*Nano Hybrid Technology Research Center, Creative and Fundamental Research Division, Korea Electrotechnology Research Institute (KERI), Changwon 51543, Republic of Korea*
[c]*Electrical Environment Research Center, Power Grid Research Division, Korea Electrotechnology Research Institute (KERI), Changwon 51543, South Korea*
[d]*Department of Biological Sciences, Pusan National University, Busan 46241, South Korea*
[e]*Busan Center, Korea Basic Science Institute (KBSI), Busan 46742, South Korea*

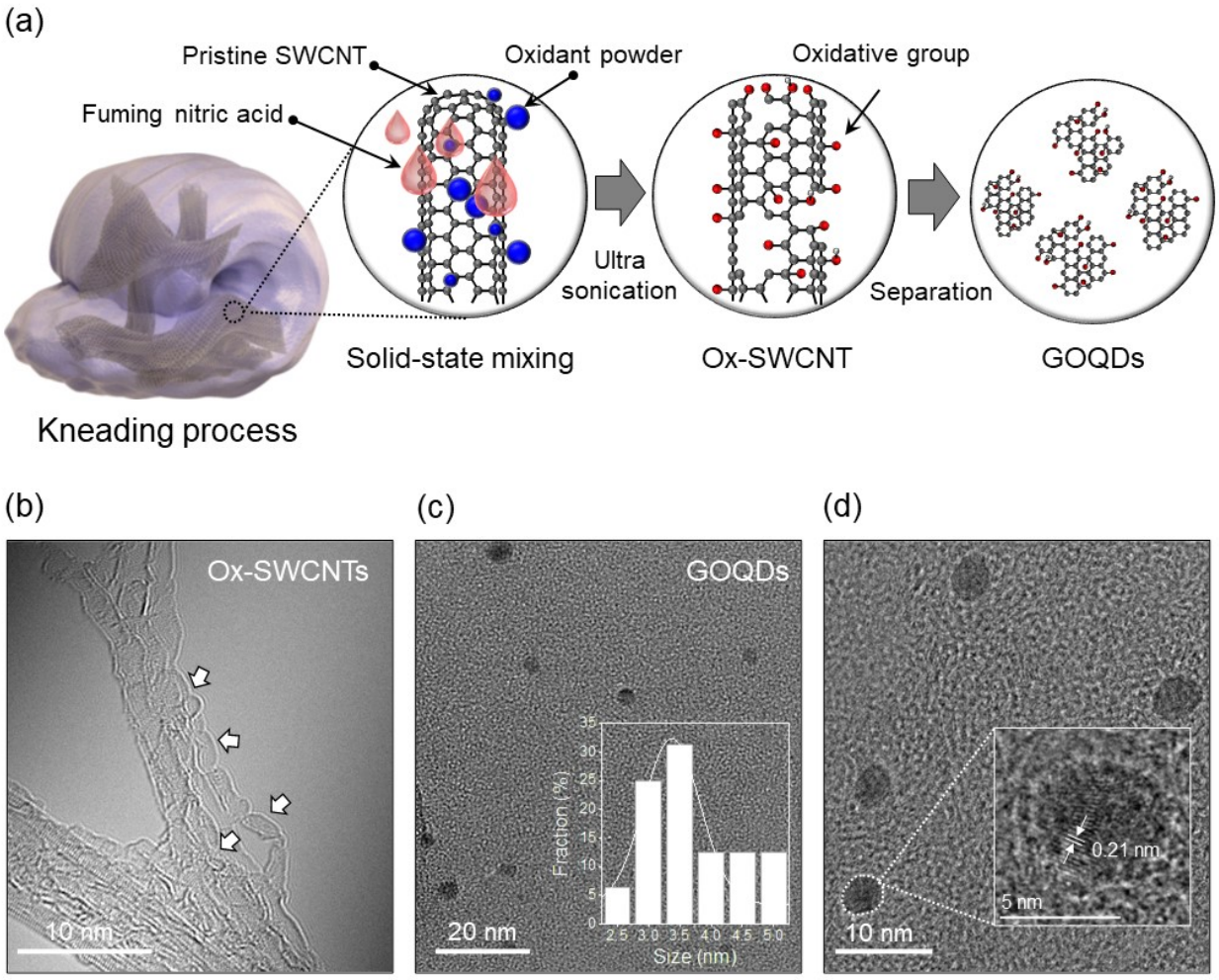

Fig S1. (a) Schematic illustration of the preparation of GOQDs from SWCNT via a direct solid-state mixing with oxidant powder and strong acids (Kneadign process). TEM image of (b) Ox-SWCNTs and (c) GOQDs. (d) HR-TEM image of GOQDs. TEM image in (b) shows oxidized nanotubes surfaces indicated by white arrow. The inset of (c) are the corresponding size distribution. The inset of (d) represent high resolution lattice images for GOQDs.

Fabrication of GOQDs powder: GOQDs were prepared from SWCNTs using chlorate-based oxidation with a kneading process. Firstly, 1 g of SWCNTs powder and 10 g of sodium chlorate ($NaClO_3$) powder were mixed with a high-speed mixer in order to distribute tiny $NaClO_3$ particles between the SWCNTs networks. This promotes the dissolution of $NaClO_3$ in the acid resulting in efficient oxidation of the SWCNTs. Then, 20 ml of the fuming nitric acid

solution was slowly dropped onto SWCNTs/$NaClO_3$ mixture powder while kneading with a Teflon spatula for a 30 min. Long-time kneading is more efficient in oxidizing carbon materials homogeneously. The mixture was kept at room temperature for 5 h; 1 L of deionized water was then added to the mixture in order to dilute the acid. Subsequently, the oxidized SWCNTs were cut into tiny graphene pieces under 750W ultrasonication for 1 h. The suspension was centrifuged at 15,000 rpm for 1 h to remove the sediment. And then, the supernatant was dialyzed in a dialysis bag of retained molecular weight of 8,000 Da for 5 days and lyophilized to get the dried GOQDs powder. At last, GOQDs suspension was prepared in deionized water with a concentration of 5 mg mL^{-1}.

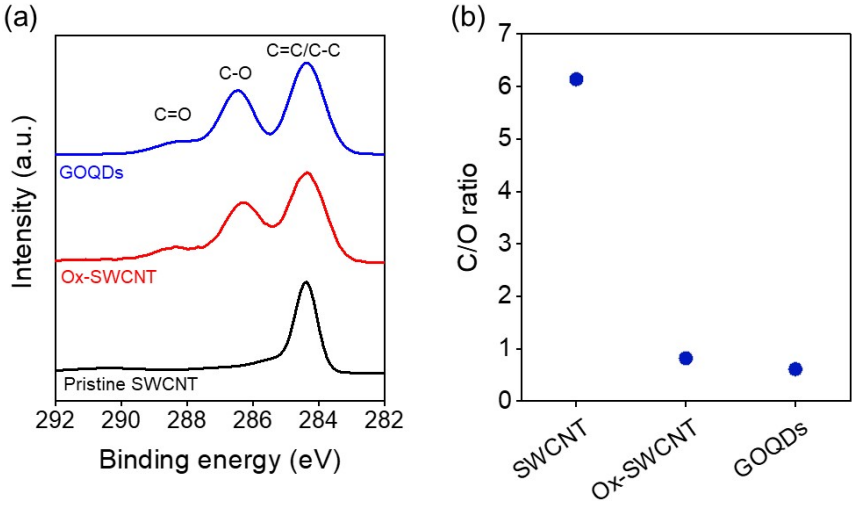

Fig S2. (a) High-resolution C1s XPS spectra of SWCNTs, Ox-SWCNTs, and GOQDs. (b) C/O ratio of SWCNTs, Ox-SWCNTs, and GOQDs.

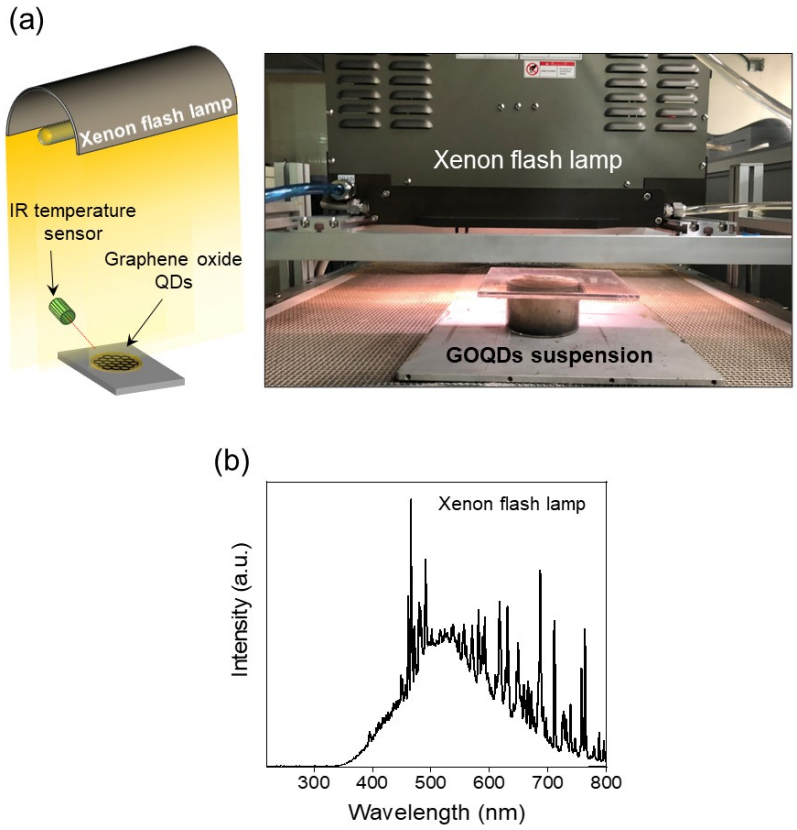

Fig S3. (a) Xenon flash lamp system. (b) Spectral distribution of flash light from xenon flash lamp.

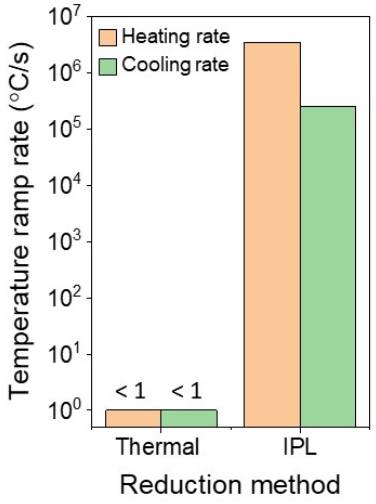

Fig S4. Heating and cooling rates of thermal and IPL treatment.

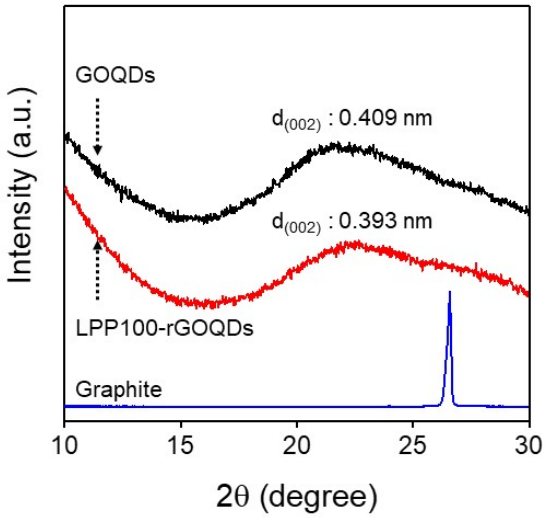

Fig S5. XRD patterns of GOQDs, LPP100-rGOQDs, and graphite.

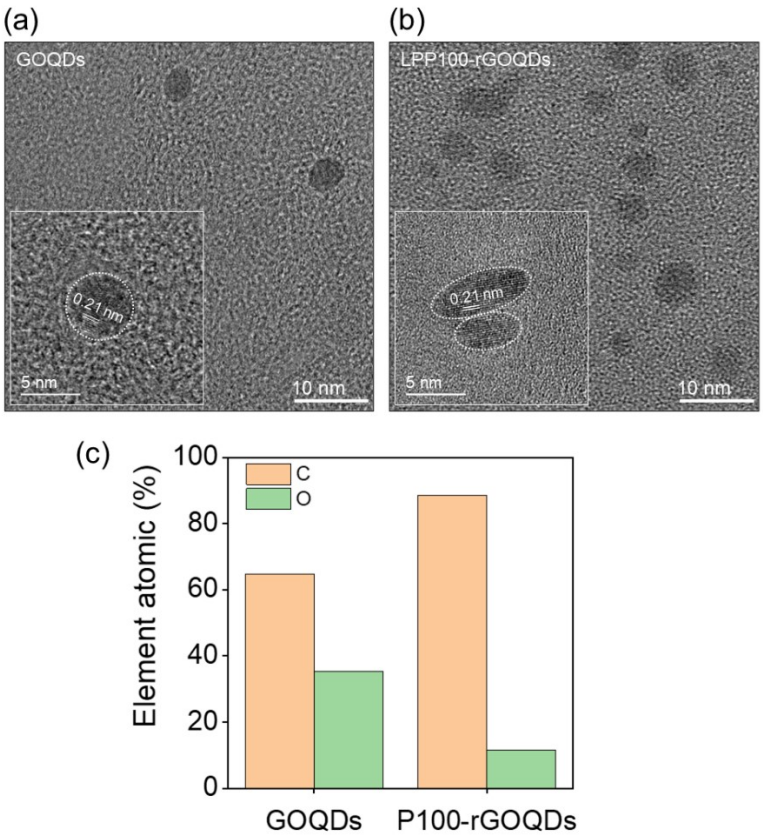

Fig S6. HR-TEM image of (a) GOQDs and (b) LPP100-rGOQDs. The inset image represents high-resolution lattice images for GOQDs and LPP100-rGOQDs. (c) Carbon and oxygen atomic percentage of GOQDs and LPP100-rGOQDs.

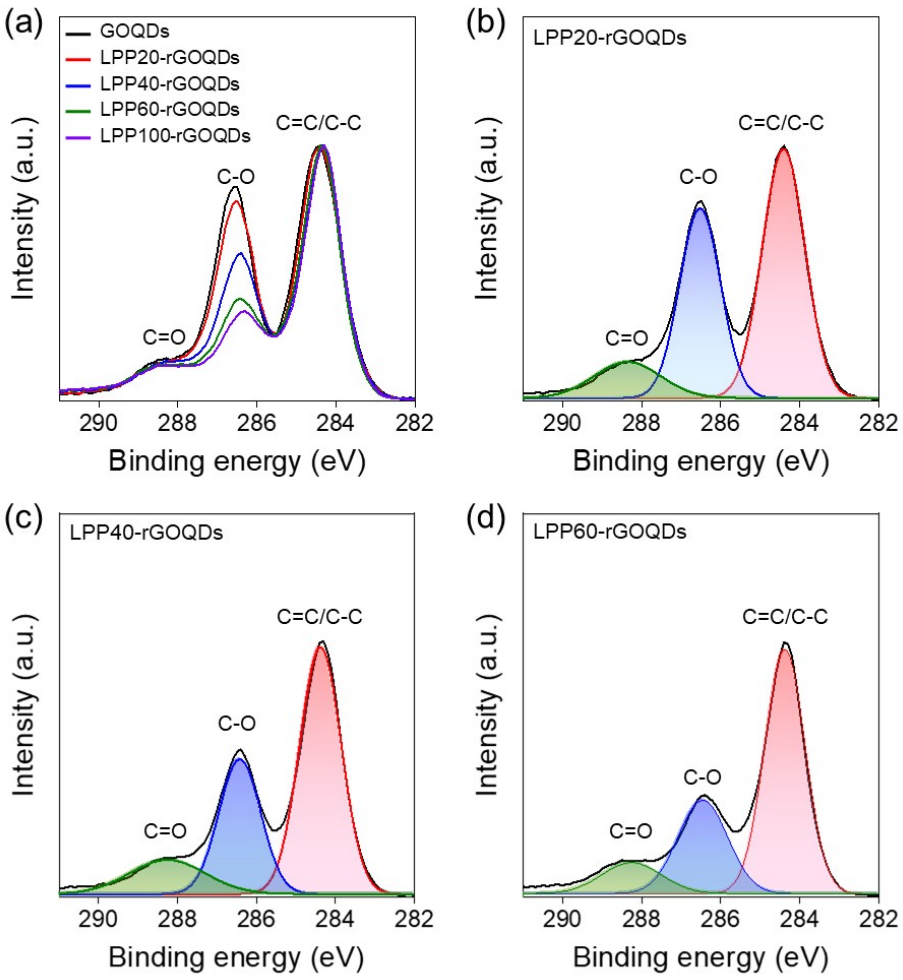

Fig S7. The XPS spectra of deconvoluted C1s peak; (a) Normalized C1s spectra of the samples, (b) LPP20-rGOQDs, (c) LPP40-rGOQDs, and (d) LPP60-rGOQDs.

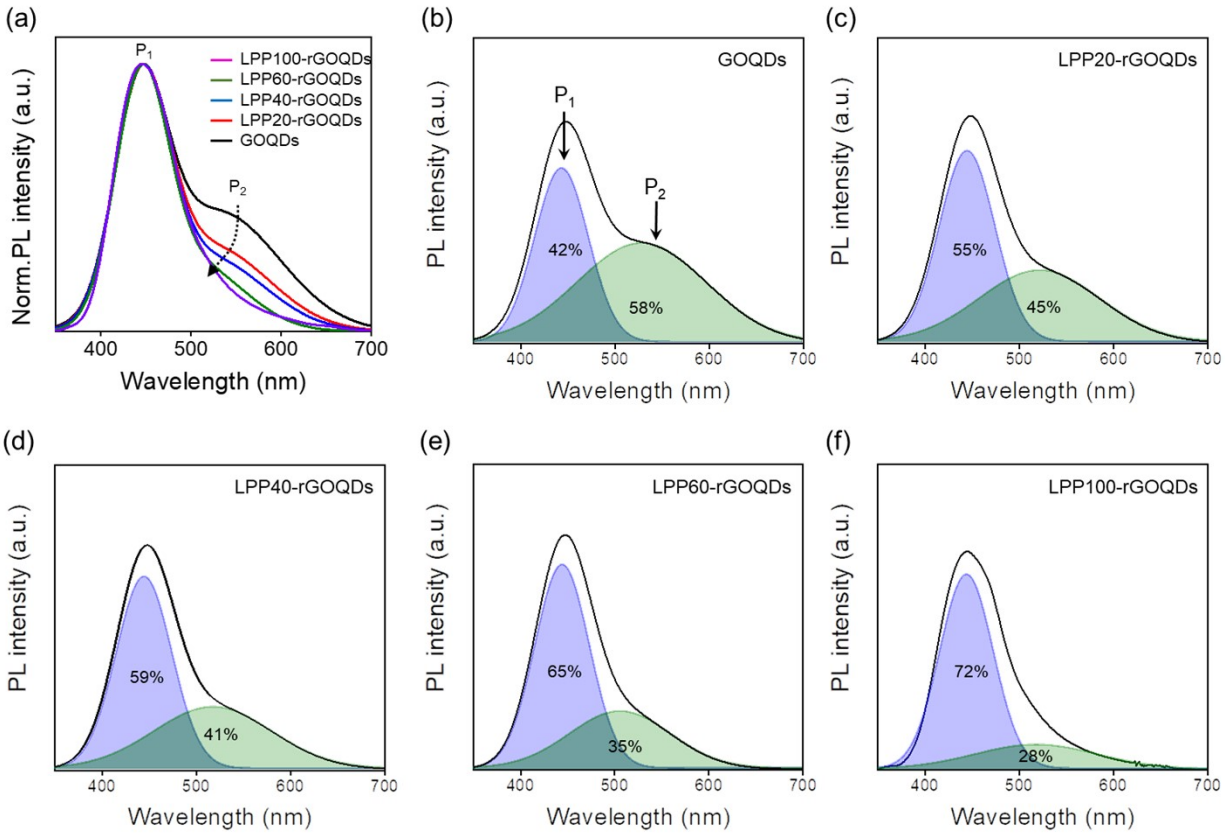

Fig S8. (a) Normalized PL spectra of GOQDs and LPP20 to LPP100-rGOQDs suspension excited at 320 nm. PL spectra with two integrated area of P_1 and P_2; (b) GOQDs and (e-f) LPP20-rGOQDs to LPP100-rGOQDs suspension.

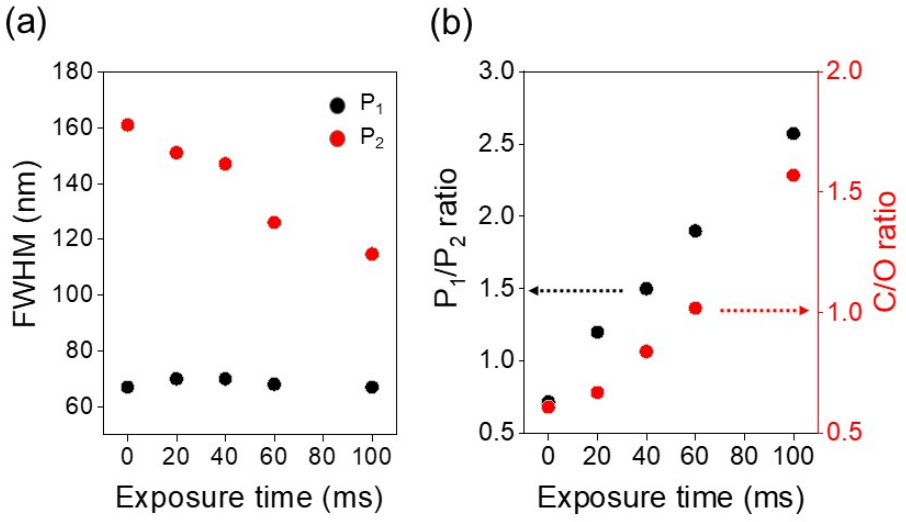

Fig S9. (a) The FWHM of P_1 and P_2 as a function of IPL exposure time. (b) Correlation of P_1/P_2 ratio with C/O ratio as a function of exposure time.

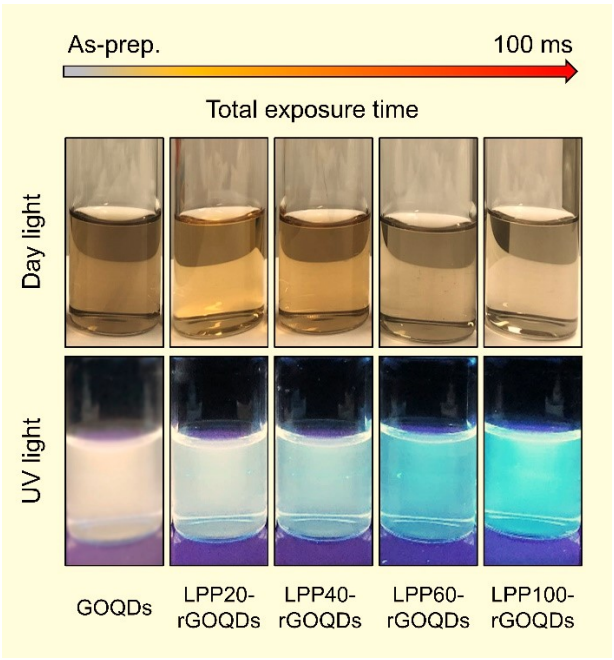

Fig S10. Photograph of GOQDs and LPP20 to LPP100-rGOQDs suspension under daylight (top view) and UV light (bottom view).

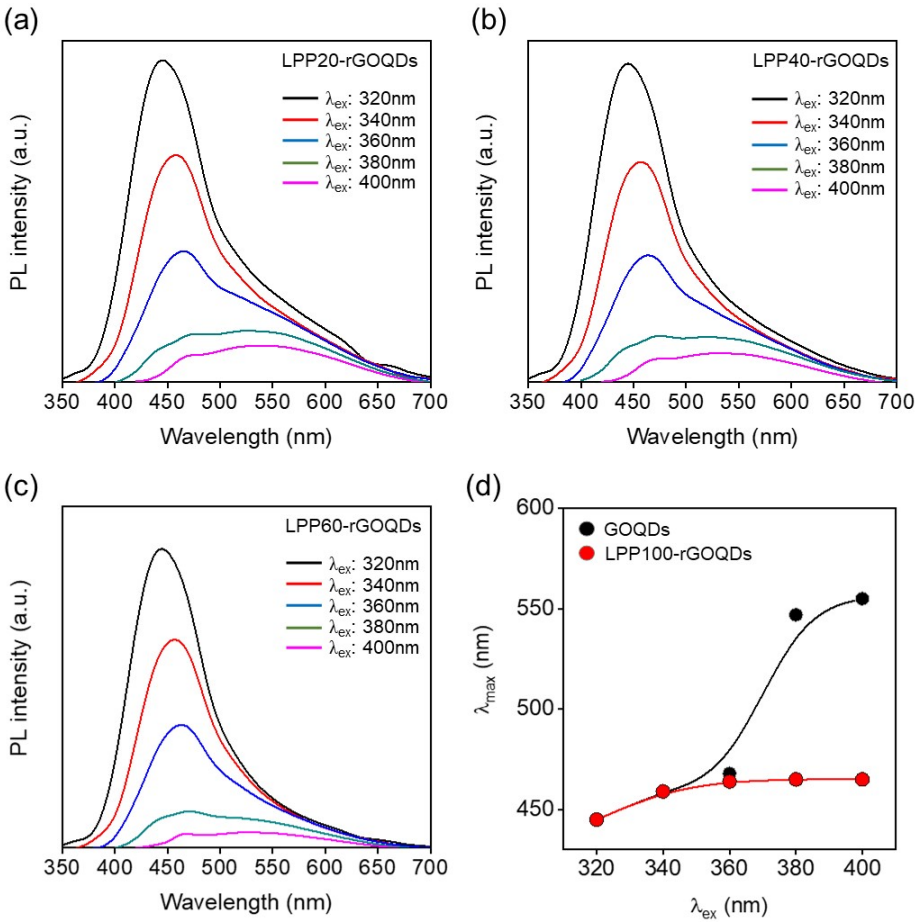

Fig S11. PL spectra of (a) LPP20-rGOQDs, (b) LPP40-rGOQDs, and (c) LPP60-rGOQDs suspensions for different excitation wavelengths. (d) The evolution of the maximal emission peak position of GOQDs and LPP100-rGOQDs at the various excitation wavelength

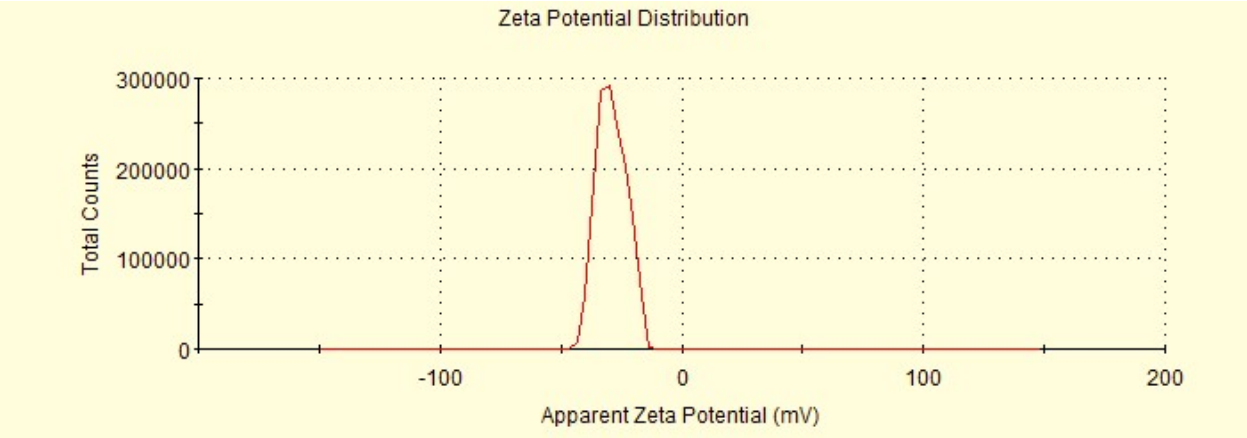

Fig S11. Zeta potential measured via dynamic light scattering (DLS) measurement of LPP100-rGOQDs

The fluorescence quantum yield of LPP-rGOQDs were calculated by comparing their integrated PL intensities and absorbance values with that of Rhodamine B in water (quantum yield is 0.31). The quantum yield of LPP-rGOQDs in water was calculated using the following equation:

$$Q = Q_R \frac{I\ OD_R n^2}{I_R\ OD\ n_R^2}$$

Where Q is fluorescence quantum yield, I is integrated fluorescence intensity, n is the refractive index of solvent (1.33 for water), and OD is the optical density (absorption). The subscript $_R$ refers to the reference fluorophore of known quantum yield. Shown below are single-point calculations of quantum yield of GOQDs and LPP20 to LPP100-rGOQDs.

	Integrated fluorescence intensity (I)	optical density (OD)	refractive index (n)	Quantum yield
Rhodamine B	580,117	0.50	1.33	0.31
GOQDs	38,924	0.52		0.02
LPP40-rGOQDs	34,209	0.50		0.02
LPP60-rGOQDs	31,956	0.51		0.02
LPP80-rGOQDs	253,869	0.50		0.13
LPP100-rGOQDs	362,666	0.51		0.19

Table S1. Quantum yield of GOQDs and LPP20 to LPP100-rGOQDs

440 nm TRPL					
Sample	As-prep.	20	40	60	100
A_1	0.86	0.85	0.86	0.85	0.89
A_2	0.14	0.15	0.14	0.15	0.11
τ_1 / ns	2.36	2.48	2.46	2.48	2.81
τ_2 / ns	10.12	11.08	11.43	12.21	14.46
τ_{ave} / ns	5.55	6.27	6.32	7.00	7.33

530 nm TRPL					
Sample	As-prep.	20	40	60	100
A_1	0.53	0.49	0.48	0.49	0.39
A_2	0.47	0.51	0.52	0.41	0.61
τ_1 / ns	1.19	1.10	0.97	0.96	0.94
τ_2 / ns	5.31	5.23	6.05	6.70	8.14
τ_{ave} / ns	3.73	3.90	4.64	5.21	7.14

Table S2. Parameters of double exponential decay function fitting

In Table S2, the lifetimes of LPP100-rGOQDs at 440nm TRPL are τ_1~2.36 ns and τ_2~14.46 ns with fractional amplitudes of 89% and 11%, respectively. The large fractional amplitude (A_1) of 89% indicates a strong influence from the excitonic recombinations with noticeably less effect from the defect-mediated recombination which is reasonable considering the observation wavelength with respect to the PL spectrum in Fig 3b. The lifetimes of LPP100-rGOQDs at 530nm TRPL are τ_1~0.94 ns and τ_2~8.14 ns with fractional amplitudes of 39% and 61%, respectively. The observable drop in the fractional amplitude associated with the excitonic recombinations from 89% at 440 nm TRPL to 39% at 540 nm TRPL is likely due to a decrease in the defect-mediated recombination at 540 nm.